Journal of Fluid Science and Technology

Vol. 3, No. 3, 2008

Verification of the Prediction Accuracy of Annual Energy Output at Noma Wind Park by the Non-Stationary and Non-Linear Wind Synopsis Simulator, RIAM-COMPACT*

Takanori UCHIDA** and Yuji OHYA**

**Research Institute for Applied Mechanics (RIAM), Kyushu University,
6-1 Kasuga-koen, Kasuga-city, Fukuoka, 816-8580, JAPAN
E-mail: takanori@riam.kyushu-u.ac.jp

Abstract

In the present study, the hub-height wind speed ratios for 16 individual wind directional groups were estimated by the RIAM-COMPACT for Noma Wind Park, Kagoshima Prefecture. The validity of the proposed estimation technique for the actual wind was examined. For this procedure, field observational data from the one year period between April, 2004 and March, 2005 were studied. In this case, the relative error on the prediction accuracy was less than 10% and less than 5% for the monthly and annual average wind speeds, respectively. Similar to the results for the annual average wind speed, the difference in the selected reference points (Wind Turbines #4 and #6) had little difference in the relative error on the prediction accuracy of the annual energy output. For both reference points, the relative error was within 10%.

Key words: RIAM-COMPACT, Complex Terrain, Wind Energy Resource, Noma Wind Park, Prediction Accuracy Verification

1. Introduction

To prevent global warming, a substantial reduction in CO_2 emissions is now considered as an urgent issue. Accordingly, the effective use of wind power energy is attracting attention as a clean and environmentally friendly energy. In Japan, the number of wind power generation facilities has been rapidly increasing to achieve the goal of 300 million KW of wind generated energy in 2010. The generated energy output from a wind turbine is proportional to the wind speed cubed. Therefore, accurate site selections with favorable wind conditions are important for constructing wind turbines, even at a pinpoint-level. Unlike the topography of Europe and North America, that of Japan is characterized mainly as complex terrain with little flat terrain. Complex terrain induces topographical effects such as flow impingement, flow separation, flow reattachment and reverse flow. These topographical effects need to be taken into consideration for selecting sites for wind turbine construction. With such a need and with the recent rapid advancement of computational capability, micro-siting software has been developed in various Japanese sectors based on Computational Fluid Dynamics (CFD)[1, 2].

Our research group has also developed a non-stationary and non-linear wind synopsis simulator, RIAM-COMPACT (Research Institute for Applied Mechanics, Kyushu University, COMputational Prediction of Airflow over Complex Terrain). This simulator is applicable for all flat and complex terrain of Japan and other countries[3]. Based on

*Received 28 Feb., 2008 (No. 08-0116)
[DOI: 10.1299/jfst.3.344]

Large-Eddy Simulation (LES), the RIAM-COMPACT simulates the wind field for a narrow targeted domain of several hundred meters to several kilometers. The main feature of the RIAM-COMPACT is its ability to predict and visualize the temporal change of topographical effects on the wind field with high accuracy. These topographical effects include flow detachment, its accompanying formation of a reverse-flow region, local speed-up and reattachment of the detached shear layer.

Observation poles of 30m tall or taller are often deployed at planned construction sites for wind power generation. Time series of meteorological data such as wind direction and speed are collected typically over a one-year period on the observation pole. If such observation data are imported into CFD so that the observation data and the CFD output results can be effectively linked together, economical provisional estimates including the annual energy output and utilized capacity can be made with high accuracy[4, 5].

In fact, we have already proposed a methodology which uses time-series data from field observations and CFD output results to estimate the actual wind speed at an arbitrary location near the location of the observational data collection[6]. Briefly, this methodology is an attempt to covert the virtual wind speed distribution (non-dimensional scales) created on the computer to the scalar wind speed of the actual scale with the use of time-series data from field observations. However, in our preceding paper[6], two issues remained unresolved: 1) the inadequate validation period of the actual wind speed and 2) the inadequate prediction accuracy of the hub-height wind speed ratio between a turbine and a reference point for individual wind directions (see Section 5). This wind speed ratio is considered as one of the key elements in the proposed methodology. Given this background, the present study will validate the proposed methodology to estimate the actual wind speed. Specifically, the wind speed ratio for each wind direction will be verified with a wind tunnel experiment for Noma Wind Park in Kagoshima Prefecture. The study will also use data collected in the field over a one-year period.

2. General Descriptions of Noma Wind Park, Kagoshima Prefecture

Noma Wind Park is situated in Minami Satsuma City in the south-west part of Kagoshima Prefecture (shown in circle in Fig.1). While the area is generally surrounded by the ocean, the west end of the cape is characterized by steep cliff-like topography with a slope angle of more than 30 degrees, which is considered typical complex terrain (Fig.2). The maximum surface elevation of the cape is 143m. On this cape, ten wind turbines of the Kyushu Electric Power, Co., Inc. have been deployed for verification testing. The rating of each individual wind turbine is 300kW, yielding a total energy output of 3,000kW from all

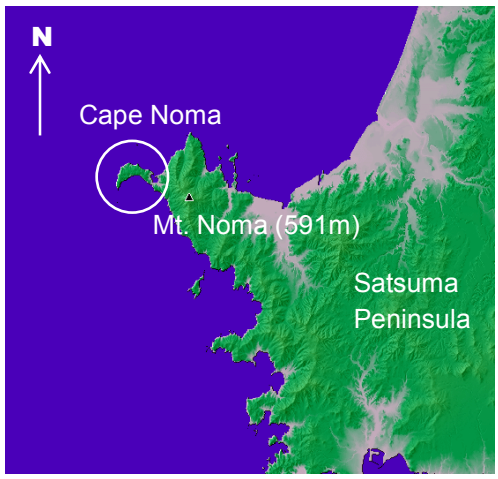

Fig.1 Topographical features of Cape Noma and its vicinity

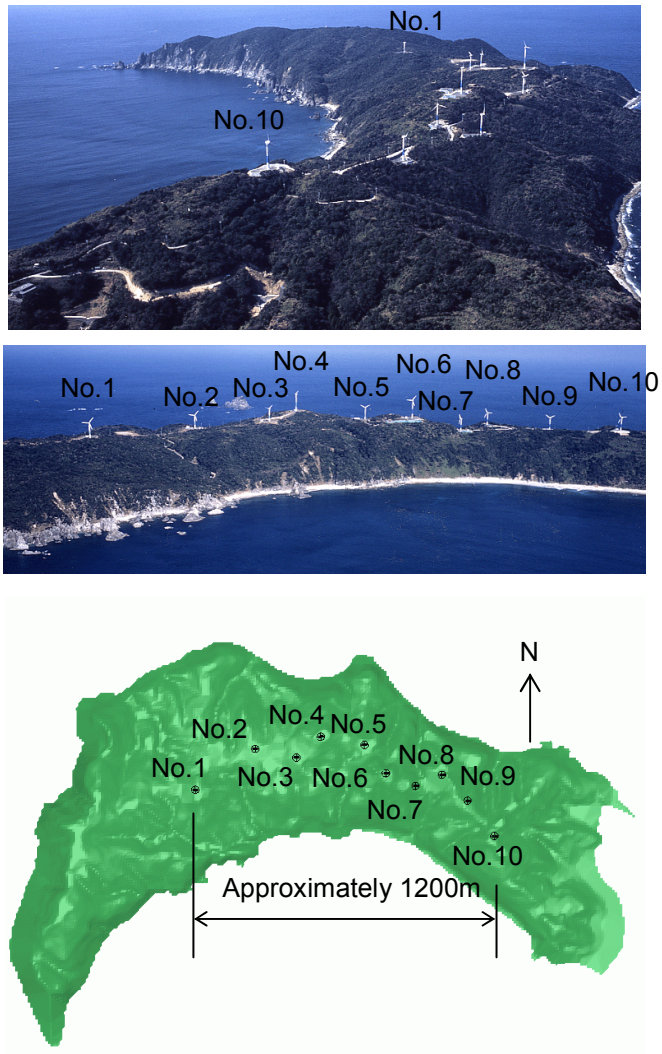

Fig.2 Appearance of Noma Wind Park

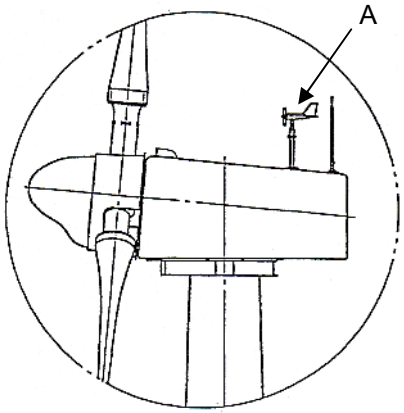

Fig.3 Prop-vane anemometer deployed on wind turbine nacelle (see A in the figure)

the turbines combined. Tables 1 and 2 show the summary of Noma Wind Park.

A prop-vane anemometer has been deployed on the nacelle of each wind turbine in Noma Wind Park as indicated by "A" in Fig.3. The time-series data observed by these prop-vane anemometers are used in the present study. The recording interval of these

Table 1 Specifications of wind turbines in Noma Wind Park

	Power Stations #1-#5	Power Stations #6-#10
Energy Output	300kW/Power Station	
Generator Types	Induction Generator	Synchronous Generator
Cut-In Wind Speeds	3.5m/s	2.5m/s
Rated Wind Speeds	14.4m/s	14.0m/s
Cut-Out Wind Speeds	24.0m/s	25.0m/s
Rotor Diameters	29m	30m
Tower Heights	30m (#4:45m)	30m (#6:45m)

Table 2 Wind turbine hub-height and surface elevation

Wind Turbine ID Number	Hub-Height (Tower height)	Surface Elevation
#1	30m	100m
#2		92m
#3		109m
#4	45m	122m
#5	30m	102m
#6	45m	117m
#7	30m	88m
#8		95m
#9		92m
#10		109m

data is 1 minute. The detailed characteristics of the wind synopsis of Noma Wind Park between June, 2002 and May, 2003 have been summarized in the literature[7]. According to this summary, the predominant wind direction at this site was from the north; the monthly average wind speed was the largest between November and March (Fig.4). Figure 5 illustrates the wind characteristics from the one-year period between April, 2004 and March, 2005. While some differences were observed for the wind speed between the two years, the occurrence frequency of the wind directions changed little between the two years.

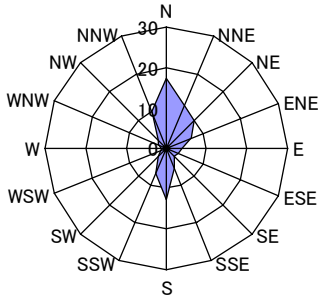

(a) Occurrence frequency of wind direction (%)

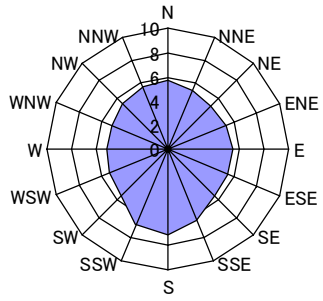

(b) Average wind speed (m/s)

Fig.4 Wind characteristics at Noma Wind Park (Wind Turbine #4) from the one-year period between June, 2002 and May, 2003

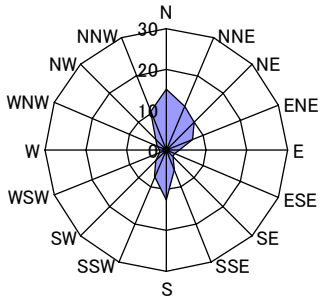

(a) Occurrence frequency of wind direction (%)

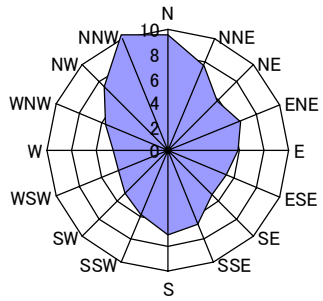

(b)Average wind speed (m/s)

Fig.5 Wind characteristics at Noma Wind Park (Wind Turbine #4) from the one-year period between April, 2004 and March, 2005.

3. Wind Tunnel Experiment for Noma Wind Park, Kagoshima Prefecture

3.1 Overview of Wind Tunnel Experiment

For the present study, an experiment was performed in a wind tunnel with thermally neutral stratification at the Research Institute for Applied Mechanics of Kyushu University. The wind tunnel is a suction type with an open circuit. The dimension of the test section of the wind tunnel is 13.5m (L) × 1.5m (W) × 1.2m (H). The wind speed can be varied between 0.5m/s and 2.0m/s. The mean turbulence intensity in the main stream direction is approximately 0.4%. To achieve uniform inflow conditions in the flow approaching to a model, the following two arrangements were made[6]. First, the scale model was deployed on an 11.5cm tall table which had been set on the floor upstream inside the wind tunnel. This arrangement was necessary to avoid the influence of the boundary layer that developed at the floor of the wind tunnel. Second, an aluminum plate with a slight slope was installed at the leading edge of the model. The use of this plate inhibited flow detachment from the leading edge of the model.

To measure airflow at the wind turbine hub-height, an I-type hot wire probe (KANOMAX Japan, Inc. 0251R-T5) and a hot-wire anemometer (KANOMAX Japan, Inc. System 7000： 1011 CTA unit, 1013 linearizer) were deployed. The hot wire probe is of the constant-temperature type. The measurement principles of this probe are as follows. A bridge circuit is constructed with a heated hot wire in the fluid being part of the circuit. From the thermal energy lost by wind blowing past the wire (unbalanced output voltage), the wind speed can be detected. A 5μm diameter tungsten wire was used as the sensing element. The time-series data in voltage were offset by 1.75V, amplified by a factor of two and low-pass filtered with a cut-off frequency of 200Hz. These data were loaded on a PC through an A/D converter board with a sampling frequency of 500Hz. The DSS for Windows by the Canopus Co., Ltd. was adopted for the data acquisition software. In the present study, only the scalar average wind speed, U(m/s), was determined from the average values of the voltage, E(V). A total of 30,000 data values were collected at each measurement point over the sampling interval (the averaging time) of 60 seconds. For probe calibrations, a sampling interval of 30 seconds was adopted. The inflow speed of the uniform flow, U, was 1.5m/s. Based on the maximum height of the model, h≈6cm, the Reynolds number ($Re=Uh/\nu$) was approximately 6×10^3. To monitor the airflow and measure the reference wind speed for calibrations of the hot-wire probe, an ultrasonic anemometer (Kaijo corporation DA-600, TR-90AH probe) was deployed.

3.2 Scale Models

In the present study, two kinds of scale models were prepared to investigate the influences of the terrain surface serrations on the airflow at the wind turbine hub-height. These scale models will be described in this subsection. The first model was prepared by stacking 1mm thick acrylic plates in a staircase pattern. The acrylic plates were cut by laser. This staircase-style scale model can be considered to model the roughness that uniformly covers the terrain surface. The second model was made of polycarbonate to create a smooth geometry without surface serrations. For simplicity, the former and the latter models will be referred as the serrated scale model and the non-serrated scale model, respectively, hereafter. Figure 6 shows magnified views of both scale models. The building process of the scale model with polycarbonate can be summarized as follows. A scale model made of polycarbonate is created with a Rapid Prototyping (RP) machine. The RP machine is able to produce a 3D model directly out of configuration data prepared by 3D CAD (3D deposition modeling). Compared to traditional methods such as hand cutting and prototype molding, RP is able to produce a prototype in a considerably smaller amount of time, which shortens the development period of a new product. RP machines use various technologies,

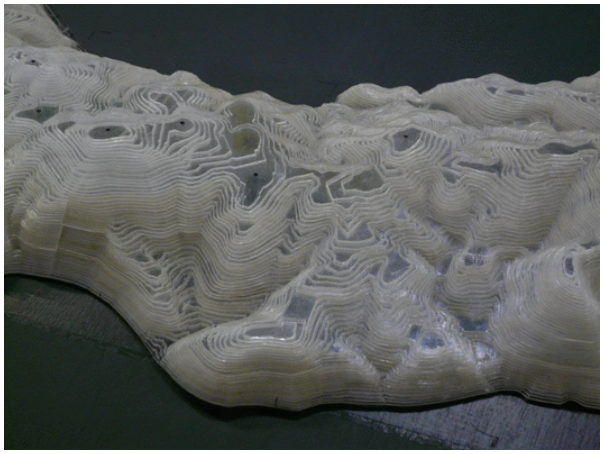

(a) Scale model with serrated surface terrain created by stacking acrylic plates of 1mm thickness

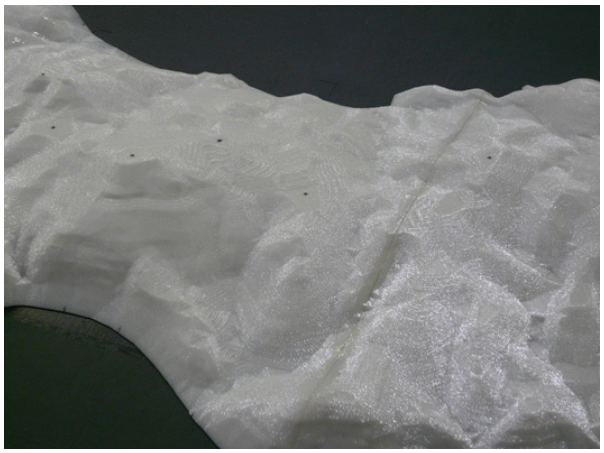

(b) Scale model without serrated surface terrain created with polycarbonate

Fig.6 Comparison of scale models. Magnified view.

which have their own unique features. For the present study, FDM-TITAN (Stratasys, Inc., U.S.A.), a model that uses "fused deposition modeling technology", was selected for use. The thickness of the individual lamination layer was 0.25mm. The outside dimension of the RP machine is 1,400mm (W) × 876mm (D) × 1,830mm (H) with a weight of 726kg. The power supply required is 230V.

The scale size of the two scale models for the present study is approximately 1/2,800. Thus, hub-heights of 30m and 45m tall in the actual scales correspond to approximately 10mm and 15mm in the wind tunnel experiment, respectively. To evaluate the average wind speed for each of the 16 wind-directional groups at the hub-height of the 10 wind turbines, the rotation of the scale model was controlled by a stepping motor with the use of a PC.

4. Numerical Simulation for Noma Wind Park, Kagoshima Prefecture

4.1 Summary of Numerical Computational Technique

For the present study, airflow over complex terrain was numerically simulated by the RIAM-COMPACT. The RIAM-COMPACT is based on a general curvilinear coordinate system with collocated grids, which avoids numerical instabilities and allows highly accurate predictions of the airflow. In the collocated grid system, the velocity components and pressure are defined at the cell center, and variables that result from the contravariant velocity components multiplied by the Jacobian are defined at the cell faces. The

computational technique of the RIAM-COMPACT is based on the Finite-Difference Method (FDM), and LES is adopted for turbulence modeling. In LES, a spatial filter is applied on the flow field to separate eddies of various sizes into Grid Scale (GS) components, which are larger than the computational grids, and SubGrid Scale (SGS) components, which are smaller than the computational grids. The large eddies, i.e. the GS components, are numerically simulated directly without the use of a physically simplified model. On the other hand, the energy dissipation by the small eddies, i.e. the SGS components, are modeled based on the physical considerations of the SGS stress. For the equations of flow, a spatially-filtered continuity equation for incompressible fluid (Eq.(1)) and a spatially-filtered version of the Navier-Stokes Equation (Eq.(2)) are used. The present study focuses on strong wind conditions with a mean wind velocity of larger than 6m/s. Therefore, effects of thermal stratification are neglected.

$$\frac{\partial \bar{u}_i}{\partial x_i} = 0 \tag{1}$$

$$\frac{\partial \bar{u}_i}{\partial t} + \bar{u}_j \frac{\partial \bar{u}_i}{\partial x_j} = -\frac{\partial \bar{p}}{\partial x_i} + \frac{1}{Re}\frac{\partial^2 \bar{u}_i}{\partial x_j \partial x_j} - \frac{\partial \tau_{ij}}{\partial x_j} \tag{2}$$

$$\tau_{ij} \approx \overline{u_i' u_j'} \approx \frac{1}{3}\overline{u_k' u_k'}\delta_{ij} - 2\nu_{SGS}\bar{S}_{ij} \tag{3}$$

$$\nu_{SGS} = \left(C_s f_s \Delta\right)^2 \left|\bar{S}\right| \tag{4}$$

$$\left|\bar{S}\right| = \left(2\bar{S}_{ij}\bar{S}_{ij}\right)^{1/2} \tag{5}$$

$$\bar{S}_{ij} = \frac{1}{2}\left(\frac{\partial \bar{u}_i}{\partial x_j} + \frac{\partial \bar{u}_j}{\partial x_i}\right) \tag{6}$$

$$f_s = 1 - exp\left(-z^+ / 25\right) \tag{7}$$

$$\Delta = \left(h_x h_y h_z\right)^{1/3} \tag{8}$$

The computational algorithm and the time marching method are based on Fractional-Step (FS) methods[8] and the Euler explicit method, respectively. The Poisson's equation for pressure is solved by the Successive Over Relaxation (SOR) method. For discretization of all the spatial terms except for the convective term in Eq.(2), a second-order central difference scheme is applied. For the convective term in Eq.(2), a third-order upwind difference scheme is applied. An interpolation technique based on 4-point differencing and 4-point interpolation by Kajishima[9] is used for the fourth-order central differencing that appears in the discretized form of the convective term. In the weighting of the numerical dispersion term of the third-order upwind differencing, α=3 is normally applied in the Kawamura-Kuwahara Scheme[10]. However, α is set to 0.5 in the present study to minimize the influence of numerical dispersion. For subgrid-scale modeling in LES, the commonly used Smagorinsky model[11] is adopted (Eq.(3)-Eq.(8)). A wall-damping function is used with a model coefficient of 0.1.

4.2 Creation and Use of High-Resolution Elevation Data

Wind disturbances (topography-induced turbulence) can be generated by slight serrations of topographic relief in the proximity of a wind turbine including those that are

too small to appear in the "50m-Gridded Elevation Data" by the Geographical Survey Institute of Japan (50m Elevation Data, hereafter). It has been reported that this type of wind disturbance may have a significant influence on energy output[12]. One plausible solution is to create elevation data with a grid spacing of 10m or less based on interpolations of the 50m Elevation Data. However, the 50m Elevation Data were generated using a 1:25,000 topographical map as the source data. Therefore, the elevation data obtained from this method may represent significantly different topography from the actual topography. In addition, the published source data is quite old. As a result, the 50m Elevation Data show a land development status significantly different from the current conditions for many of the planned construction sites for wind turbines. The renewal time of the 50m Elevation Data remains unknown.

With these various issues in mind, we have proposed a methodology to construct detailed topography of 10m or less in spatial resolution, even as low as 2 - 5m[13]. In this methodology, CAD data in the DXF format or a paper-based map of 1:2,500 - 1:10,000 are linked to the Geographical Information System (GIS). Figure 7 illustrates the appearance of a three-dimensionalized area constructed from a paper drawing of 1:2,500 (2D) that was scanned by a large scanner. Only a few days are required to construct the elevation data from a paper map. Figure 8 shows comparisons of the elevation data of various spatial resolutions for the same topography (Noma Cape, Kagoshima Prefecture; maximum elevation: 143m). Figure 8(a) shows the 500m resolution data, which are used for New Energy and Industrial Technology Development Organization (NEDO) wind maps. Figure 8(b) shows the 50m resolution data that are commonly used for selecting sites for wind power generation. Figure 8(c) shows the 5m resolution data that can be constructed from the methodology proposed in the present study. The difference in the representation of the topography is evident. In Fig.8(a), even the basics of the topography are hardly reconstructed. To the contrary, the topography down to subtle details has been reconstructed with high precision in Fig.8(c). Selection of a site appropriate for wind power generation at the pin-point level depends on the representation of the actual complex topography on the computer. In other words, such site selection relies heavily on the accuracy of the terrain used as the surface boundary condition. If the representation of the topography is sufficiently accurate, the flow field can be reconstructed with very high accuracy by the RIAM-COMPACT.

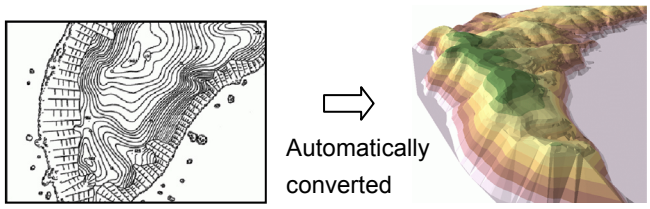

Fig.7 Digitalization (3D) of paper-based drawing (2D)

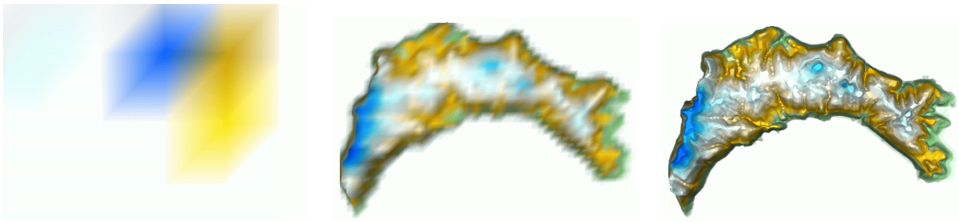

(a)500m (b)50m (c)5m

Fig.8 Comparisons of spatial resolutions for Cape Noma

4.3 Computational Conditions

For the present study, the computational domain was set to a 5km square with wind turbine #4 in the center (Fig.2). The top of the computational domain was set to 700m. The above-mentioned high-resolution elevation data with 5m spatial resolution were used for the elevation data. The number of grid points was 51 × 51 × 41 for the main-stream direction (x), the cross-stream direction (y), and the vertical direction (z), respectively. The grid widths in the x- and y-directions were varied so that the grid density increased toward the center of the computational domain. The grids in the z-direction were also unevenly spaced so that the grids were concentrated near the ground surface. The vertical height of the first layer of grid cells, that is the minimum vertical grid height, was approximately 2.5m. A wind speed profile based on the 1/7 power law was given for the inflow boundary. Slip conditions were set for the lateral and upper boundary. Convective outflow conditions were applied for the outflow boundary surface. On the ground, the non-slip condition was imposed. The non-dimensional variable, Re in Eq.(2), defined as $U_{in}h/\nu$ in this study, was set to $Re(=U_{in}h/\nu)=10^4$ [14]. Figure 9 shows representative scales used for the present computations. The variable, h, indicates the surface elevation difference of the computational domain (h=143m). The variables, U_{in} and ν represent the wind speed at the maximum surface elevation at the inflow boundary and the kinematic viscosity, respectively. The time interval, Δt, was set to $2\times10^{-3}h/U_{in}$.

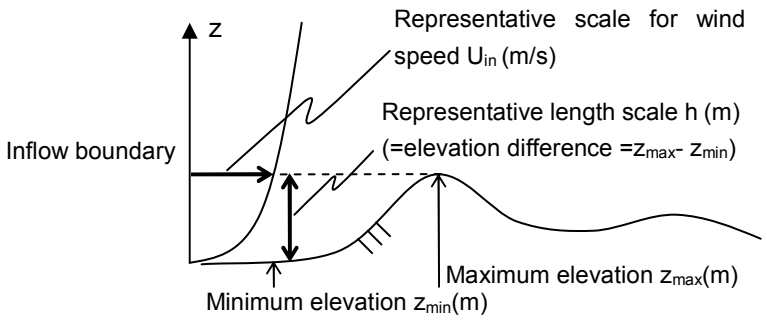

Fig.9 Representative scales for the present calculations

4.4 Discussions: Comparisons of Wind Speed Ratios at the Wind Turbine Hub-Height

Figure 10 illustrates the vertical cross-sectional views of the wind velocity vectors that pass through wind turbines #1 and #4. Local enhancement of the airflow velocity at the hub-height is evident.

The wind speed ratio at the wind turbine hub-height for each of the 16 wind directional groups was investigated for the 10 wind turbines. As examples, the wind speed

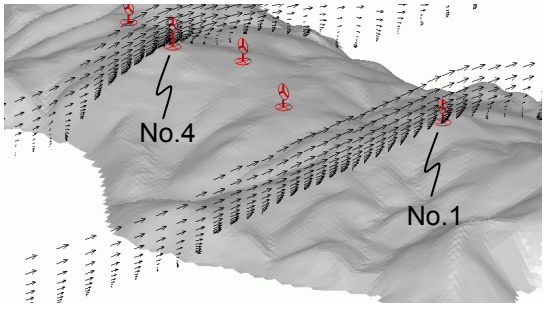

Fig.10 Vertical cross-sectional views of velocity vectors that pass through wind turbines #1 and #4

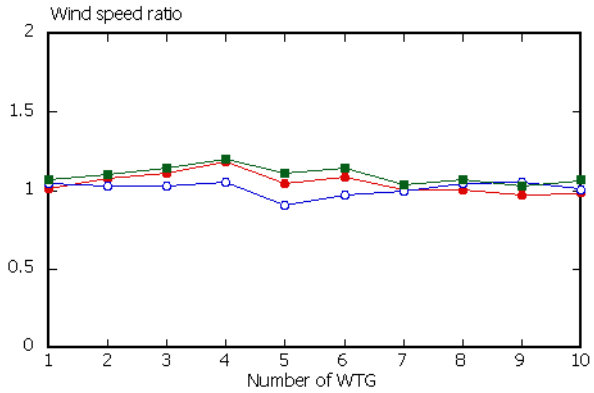

(a) Case of northerly wind

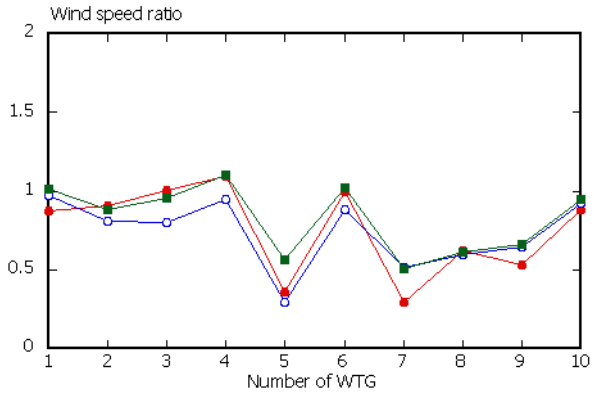

(b) Case of west northwesterly wind

Fig.11 Comparisons of wind speed ratio at wind turbine hub-height
Red: wind tunnel experiment with "serrated scale model", blue: wind tunnel experiment with "non-serrated scale model", green: numerical simulation with RIAM-COMPACT

ratios from the northerly and west northwesterly cases are shown in Fig.11. The wind speed ratio at the wind turbine hub-height was defined for the wind tunnel experiment as: average wind speed at each wind turbine height / inflow wind speed at z = 50mm at turntable center. Numerical simulations were performed under the identical conditions as for the wind tunnel experiment. The wind speed ratio was calculated from the wind speed simulated for the locations that corresponded to the relevant measurement locations in the wind tunnel experiment. In Fig.11, the red and blue symbols indicate the results from the wind tunnel experiment with the serrated and non-serrated scale models, respectively. The green symbol indicates the simulated result from the RIAM-COMPACT. Even for a given wind directional group, the wind speed ratio sometimes varies significantly depending on the wind turbine positions (Fig.11b). For both the northerly and west northwesterly cases, the results from the wind tunnel experiment and the numerical simulations by the RIAM-COMPACT agreed remarkably well. For the other wind directional groups, the results from the wind tunnel experiment and the numerical simulations showed similar agreement. This finding suggests that both the wind tunnel experiment and the numerical simulations were operated with high accuracy; and that numerical simulations by the RIAM-COMPACT are valid as an alternative tool to wind tunnel experiments. Finally, no obvious influences of topographical serrations were found on the airflow at the wind turbine hub-height in the present wind tunnel experiment with scale models of approximately 1:2,800.

5. Technique to Estimate the Actual Wind Speed at Noma Wind Park, Kagoshima Prefecture

5.1 Summary of Procedure

A procedure to estimate the time-series wind speed data (the time-series of scalar wind speed) for an arbitrary location over complex terrain is explained below. This procedure requires time-series data acquired in field observations and CFD output results (the time-averaged wind field).

Step 1.

As illustrated in Fig.12, wind simulations are performed by the RIAM-COMPACT for 16 individual wind directional groups for the site of interest. After the flow field has been sufficiently developed, computations are continued to obtain the time-average of the flow field.

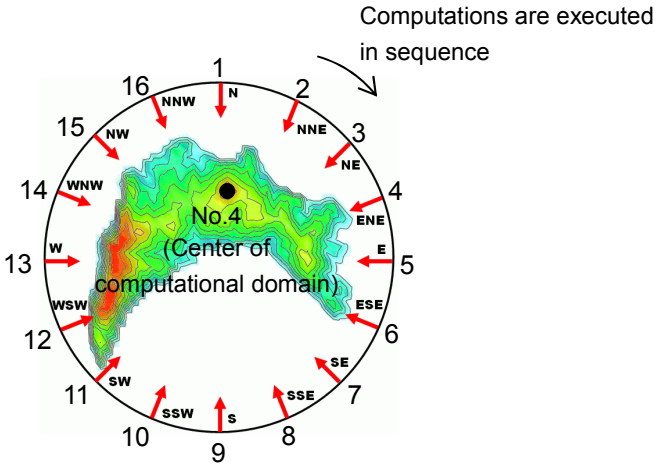

Fig.12 Conceptual view of wind simulation from 16 wind directional groups for Noma Wind Park

Step 2.

For each inflow directional group, the ratio of the hub-height wind speed of the evaluation point to the wind speed at the observation pole height (i.e., a reference point) is computed, yielding 16 sets of wind speed ratios (Fig.12). The value of the wind speed at the reference point is normalized as "1." Here, the wind direction set at the inflow boundary is assumed to match with that at the reference point. In the present study, Wind Turbines (WTs) #4 and #6 were used as reference points, thus the following wind speed ratios were evaluated: WT #1/WT #4, WT #2/WT #4, WT #3/WT #4, WT #5/WT #4 …, WT #10/WT #4; WT #1/WT #6, WT #2/WT #6, WT #3/WT #6, #4/WT #6, WT #5/WT #6, WT #7/WT #6, …, WT #10/WT #6. All the above wind speeds correspond to scalar wind speeds, VEL, which are computed with the use of the time-averaged wind velocity components for the x- and y-directions as

$$VEL = \sqrt{\left(\overline{U}^2 + \overline{V}^2\right)} \tag{9}$$

Step 3.

Observational data from the reference point are multiplied by the corresponding wind speed ratio according to the reference-point wind direction at the time of observation. The relevant wind speed ratios are estimated in advance. Thus, a time-series of observational data from the reference point are converted to a time-series of data (scalar wind speed) for

Table 3 Wind speeds and energy generation for the entire Noma Wind Park for the one-year period between April, 2004 and March, 2005.

	Reference Turbine: Turbine #4						Reference Turbine: Turbine #6					
	Average Wind Speed (m/s)			Total Energy Output (kWh)			Average Wind Speed (m/s)			Total Energy Output (kWh)		
	Observed value	Predicted Value	Error (%)	Observed value	Predicted Value	Error (%)	Observed value	Predicted Value	Error (%)	Observed value	Predicted Value	Error (%)
2005.1	8.6	8.8	2.3	829,314	789,416	4.8	8.6	8.7	1.2	804,707	765,338	4.9
2	8.4	8.5	1.2	629,857	602,927	4.3	8.4	8.6	2.4	641,344	625,842	2.4
3	7.4	7.8	5.4	593,338	600,989	1.3	7.4	7.8	5.4	620,940	623,478	0.4
2006.4	5.7	6.0	5.3	426,880	395,223	7.4	5.8	5.8	0.0	422,092	380,317	9.9
5	5.3	5.8	9.4	389,130	373,972	3.9	5.4	5.5	1.9	380,793	360,903	5.2
6	4.9	5.1	4.1	294,355	260,822	11.4	4.9	5.1	4.1	286,042	285,807	0.1
7	4.5	4.7	4.4	194,153	174,561	10.1	4.5	4.4	5.9	187,834	157,923	15.9
8	4.5	4.8	6.7	229,636	215,607	6.1	4.5	4.7	4.4	223,184	217,204	2.7
9	–	–	–	–	–	–	–	–	–	–	–	–
10	7.7	8.4	9.1	229,936	235,981	2.6	7.9	7.7	2.5	202,660	184,202	9.1
11	6.1	6.3	3.3	385,875	384,512	0.4	6.2	5.9	4.8	369,633	325,222	12.0
12	6.1	6.2	1.6	410,712	372,127	9.4	6.2	6	3.2	402,237	346,704	13.8
Annual Averages	5.8	6.0	3.4	4,613,187	4,406,138	4.5	5.8	5.9	1.7	4,541,465	4,272,940	5.9

the evaluation point. This operation can be applied for time-series of observational data over one year or any period of time. By combining this operation with statistical processing, the monthly and annual average values of the wind speed can be obtained for an arbitrary point of evaluation.

5.2 Computational Results and Discussions

Based on simulations of wind speed for the 16 wind directional groups, the monthly and annual averages of wind speed were examined for two cases. In the first case, the values of the wind speeds for turbines #1 to #10 were predicted with the use of the wind direction and speed data from the nacelle on turbine #4 (Elevation: 122m, Hub-height: 45m) as the reference-point data. In the second case, the values of the wind speeds for turbines #1 to #10 were predicted with the use of the wind direction and speed data from the nacelle on turbine #6 (Elevation: 117m, Hub-height: 45m) as the reference-point data. The results are shown in Table 3. The wind speeds in Table 3 represent those for the entire Noma Wind Park and were obtained by averaging relevant values from individual wind turbines.

Differences in the predicted values of the wind speed using the two reference points (turbine #4 and turbine #6) were insignificant. In the present case, the horizontal separation and the surface elevation difference between the two reference points were less than 1km and 50m, respectively. In this case, the relative error of the prediction accuracy was within 10% for the monthly average wind speed and within 5% for the annual average wind speed.

The predicted values of the annual energy output were examined. Using a turbine power curve, the hub-height wind speed predicted by the RIAM-COMPACT was converted to energy output. The energy output was integrated to predict the annual energy output. The predicted values of energy output are shown in Table 3. Comparisons between the values of energy output measured in the field and those predicted by the RIAM-COMPACT indicate a similar result as for the comparisons of the annual average wind speed. That is, the relative error for the prediction accuracy was within 10% for both reference points (Turbines #4 and #6), thus the choice of reference points had little influence on the relative error of the prediction accuracy.

Characteristics of airflow over complex terrain are discussed in the previous literature[6] and support the estimation technique of the actual wind speed proposed in this study. These characteristics are restated here. The time-series data from turbine #1 and turbine #10 from February 2003 were compared. This comparison revealed quite similar temporal variations of the monthly average values of wind speed between the two turbines although they were horizontally and vertically separated by 1,200m and 9m, respectively (Refer to Fig.2 and Table 2). A scatter diagram of the corresponding data yielded a

correlation coefficient of 0.84. A similar trend was found from the observational data collected over one year at the two turbines. Furthermore, the wind speeds were estimated for the two turbines using the observational data and the wind speed ratios that were computed by the CFD for the 16 wind directional groups. These estimated wind speeds also showed good agreement throughout the year. All these results are considered to have led to the agreement of the relevant values in Table 3.

In summary, scalar wind speed at an arbitrary point near the reference point can be estimated with high accuracy if 1) the influences of small variations of topographical relief on the wind are included in the CFD and 2) the wind ratios between the reference point and an arbitrary point of evaluation are computed.

6.Concluding Remarks

In the present study, the hub-height wind speed ratios for 16 individual wind directional groups were estimated by the RIAM-COMPACT for Noma Wind Park, Kagoshima Prefecture. The RIAM-COMPACT is a non-stationary and non-linear wind synopsis simulator based on a general curvilinear coordinate system with collocated grids. The estimated hub-height wind speed ratios were verified with the results from a wind tunnel experiment. To investigate the influence of a serrated terrain-surface on the airflow at the hub-heights of wind turbines, two types of scale models were created.

The results from the wind tunnel experiments and the numerical simulations with the RIAM-COMPACT agreed extremely well. For a given wind directional group, the wind speed ratio changed significantly in some cases according to the wind turbine position. The present wind tunnel experiment was performed with scale models of approximately 1:2,800. In this case, no significant influences of serrations of the terrain surface were found for the airflow at the wind turbine hub-heights.

The validity of the proposed estimation technique for the actual wind was examined. For this procedure, field observational data from the one year period between April, 2004 and March, 2005 were studied. When the values of wind speed obtained for individual wind turbines were combined together as the values for the entire Noma Wind Park, the selection of the reference points (Wind Turbines #4 and #6) caused insignificant differences on the value of wind speed for the entire Noma Wind Park. In the present case, the horizontal and vertical separation distances between the two turbines were less than 1km and less than 50m, respectively. In this case, the relative error on the prediction accuracy was less than 10% and less than 5% for the monthly and annual average wind speeds, respectively.

Similar to the results for the annual average wind speed, the difference in the selected reference points (Wind Turbines #4 and #6) had little difference in the relative error on the prediction accuracy of the annual energy output. For both reference points, the relative error was within 10%.

Acknowledgement

The present research was funded by the project on “Development of technology for detailed construction of terrain with spatial resolutions of less than 10m and its application for visual evaluations of wind disturbances at wind turbine hub-height” (Principle Investigator: Takanori Uchida). This project was administered by the New Energy and Industrial Technology Development Organization (NEDO) as one of the Industrial Technology Research Grant Projects of 2006 (January, 2006 – December, 2008). Observational data from the Noma Wind Park were provided by Kyushu Electric Power, Co., Inc. and West Japan Engineering Consultants, Inc. (West JEC). The authors would like to express their gratitude to all the above-mentioned organizations.

References

(1) Murakami, S., Mochida, A., Kato, S. and Kimura, A., Development and Verification of Local Area Wind Energy Prediction System LAWEPS, J. Japan Society of Fluid Dynamics, (in Japanese), Vol.22, No.5 (2003), pp.375-386.
(2) Ishihara, I., A Nonlinear Wind Prediction Model MASCOT: Development and Application, J. Japan Society of Fluid Dynamics, (in Japanese), Vol.22, No.5 (2003), pp.387-396.
(3) Uchida, T. and Ohya, Y., Development of the Local Wind Field Simulator RIAM-COMPACT—Wind Field Assessment and Real Time Simulation—, J. Japan Society of Fluid Dynamics, (in Japanese), Vol.22, No.5 (2003), pp.417-428.
(4) Otsuka, K. et al., A Wind Prediction Method Based on Observation, Proceedings of the 26th wind power energy use symposium, (in Japanese), (2004), pp.227-230.
(5) Hashimoto, A. et al., Proceedings of the 29th wind power energy use symposium, (in Japanese), (2007), pp.275-278.
(6) Uchida, T. and Ohya, Y., Proposal of Real Wind Speed Prediction Method over Complex Terrain by Using CFD, Journal of Applied Mechanics JSCE, (in Japanese), Vol.10 (2007), pp.733-740.
(7) Uchida, T. and Ohya, Y., Flow Characteristics over Complex Terrain Measured with Anemometer Equipped with Nacelle—For the Case of Cape—, Reports of Research Institute for Applied Mechanics, Kyushu University, (in Japanese), Vol.130 (2006), pp.35-52.
(8) Kim, J. and Moin, P., Application of a fractional-step method to incompressible Navier-Stokes equations, J. Comput. Phys., Vol.59 (1985), pp.308-323.
(9) Kajishima, T., Upstream-shifted interpolation method for numerical simulation of incompressible flows, Bull. Japan Soc. Mec. Eng. B, (in Japanese), 60-578 (1994), pp.3319-3326.
(10) Kawamura, T., Takami, H. and Kuwahara, K., Computation of high Reynolds number flow around a circular cylinder with surface roughness, Fluid Dyn. Res., Vol.1 (1986), pp.145-162.
(11) Smagorinsky, J., General circulation experiments with the primitive equations, Part 1, Basic experiments, Mon. Weather Rev., Vol.91 (1963), pp.99-164.
(12) Uchida, T., Ohya, Y., Micro-siting Technique for Wind Turbine Generator by Using High Resolution Elevation Data, JSME International Journal「Environmental Flows」, Series B, Vol.49, No.3 (2003), pp.567-575.
(13) Uchida, T., Ohya, Y., Araya, R., Tanabe, M. and Kawashima, Y., Construction of High Resolution Elevation Data from Paper Map for Numerical Model “RIAM-COMPACT”, Reports of Research Institute for Applied Mechanics, Kyushu University, (in Japanese), Vol.129 (2005), pp.135-141.
(14) Kato, M., Special Edition Toward More Intelligent Experiments on Fluid Dynamics. Present and Future on Testing Similarities Related to Fluid and Structures Interaction. Comparison between Model Experiments and Prototype Behavior. part2. Wind tunnel simulation of atmospheric turbulence over complex terrains, Wind Engineers, JAWE, (in Japanese), No.59 (1994), pp.89-92.